

Cite this: DOI: 00.0000/xxxxxxxxxx

Supplementary Information for *The destruction of $^3\text{HeT}^+$ in collisions with tritium: A dynamical study*

Jayakrushna Sahoo^a, Duncan Bossion^b, Felix Spanier^c, Tomás González-Lezana^{d*}, and Yohann Scribano^{a†}

The present Supplementary Information contains:

- Table 1 with the parameters for the ABC calculation.
- Table 2 with the parameters for the QCT calculation.
- Figure 1 with the integral cross section as a function of the collision energy obtained with the three methods.
- Figure 2 with the integral cross sections for the $\text{T}+^3\text{HeT}(v=0, j=0-5)^+ \rightarrow \text{T}_2^++^3\text{He}$ reaction obtained with the SQM method.
- Figure 3 with the integral cross sections for the $\text{T}+^3\text{HeT}(v=0, j=0-5)^+ \rightarrow \text{T}_2^++^3\text{He}$ reaction obtained with the QCT method.
- Figure 4 with the rate constants for the $\text{T}+^3\text{HeT}(v=0, j=0-5)^+ \rightarrow \text{T}_2^++^3\text{He}$ reaction obtained with the QCT method.
- Figure 5 with the rate constants for the $\text{T}+^3\text{HeT}(v=0, j=0-5)^+ \rightarrow \text{T}_2^++^3\text{He}$ reaction obtained with the QCT method.
- Figure 6 with the thermal rate constants obtained from those for the $\text{T}+^3\text{HeT}(v=0, j=0-5)^+ \rightarrow \text{T}_2^++^3\text{He}$ reaction obtained with the SQM and QCT methods.
- Figure 7 with the rotational distributions for the $\text{T}+^3\text{HeT}(v=0, j=0)^+ \rightarrow \text{T}_2^++^3\text{He}$ reaction at $E_c = 10$ meV.
- Figure 8 with the final state-resolved differential cross sections at $E_c = 10$ meV for the $\text{T}+^3\text{HeT}(v=0, j=0)^+ \rightarrow \text{T}_2^++^3\text{He}$ reaction.

Table 1 Values of the parameters for used in the ABC code for the calculation with $^3\text{HeT}^+$ ($v=0, j=0$).

E_c range (eV)	j_{\max}	E_{\max} (eV)	ρ_{\max} (a_0)	n_{sec}	J_{\max}	Ω_{\max}
$10^{-5} - 10^{-4}$	30	1.4	150	3723	9	9
$10^{-4} - 10^{-3}$	32	1.4	120	2973	15	10
$10^{-3} - 10^{-2}$	32	1.4	80	1315	25	7
$10^{-2} - 10^{-1}$	34	1.6	40	486	48	10

Table 2 Parameters for $^3\text{HeT}^+$ ($v=0, j=0$) used for the QCT calculations. Maximal impact parameter is in bohr and N_t represents the total number of trajectories.

E_c range (eV)	b_{\max}	N_t
$10^{-5} - 10^{-4}$	67.6 – 38.8	10000
$10^{-4} - 10^{-3}$	38.8 – 22.4	10000
$10^{-3} - 10^{-2}$	22.4 – 13.2	20000
$10^{-2} - 10^{-1}$	13.2 – 10.3	20000
$10^{-1} - 10^0$	13.2 – 8.7	30000

^a Laboratoire Univers et Particules de Montpellier, Université de Montpellier, UMR-CNRS 5299, 34095 Montpellier Cedex, France

^b IPR—Université de Rennes Bât 11b, Campus de Beaulieu, 263 Avenue du Général Leclerc, 35042 Rennes Cedex, France

^c Institut für Theoretische Astrophysik, Universität Heidelberg, Albert-Ueberle-Str. 2 und Philosophenweg 12, 69120 Heidelberg, Germany

^d Instituto de Física Fundamental, IFF-C.S.I.C., Serrano 123, Madrid 28006, Spain

* E-mail: t.gonzalez.lezana@csic.es

† E-mail: yohann.scribano@umontpellier.fr

* Part of Festschrift Honouring Prof. N. Sathyamurthy's 75th birthday

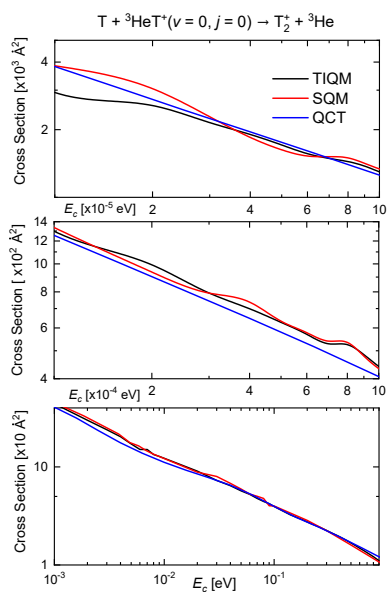


Fig. 1 Integral cross sections obtained with the TIQM (black), SQM (red) and QCT (blue) approaches for the $T + {}^3\text{HeT}^+(v=0, j=0) \rightarrow T_2^+ + {}^3\text{He}$ reaction separated in different log-scale decades for the energy: Top panel is between 10^{-5} and 10^{-4} eV; mid panel is between 10^{-4} and 10^{-3} eV and bottom panel is between 10^{-3} and 1 eV. Also notice factors for the cross sections in the y-axis.

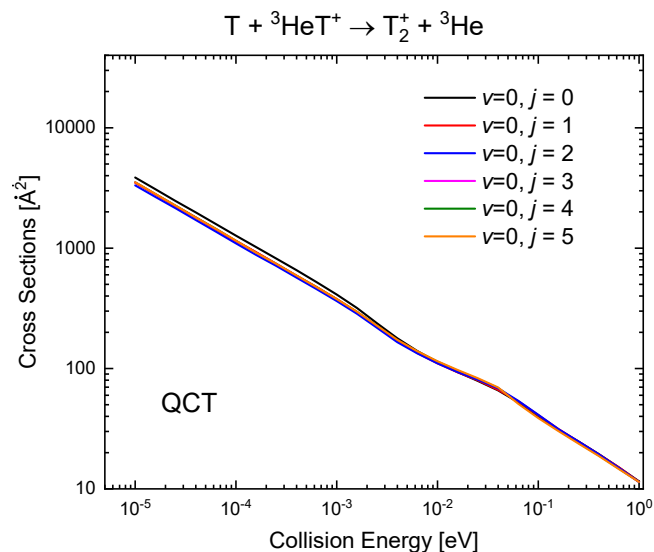


Fig. 3 Same as Figure 2 obtained with the QCT approach.

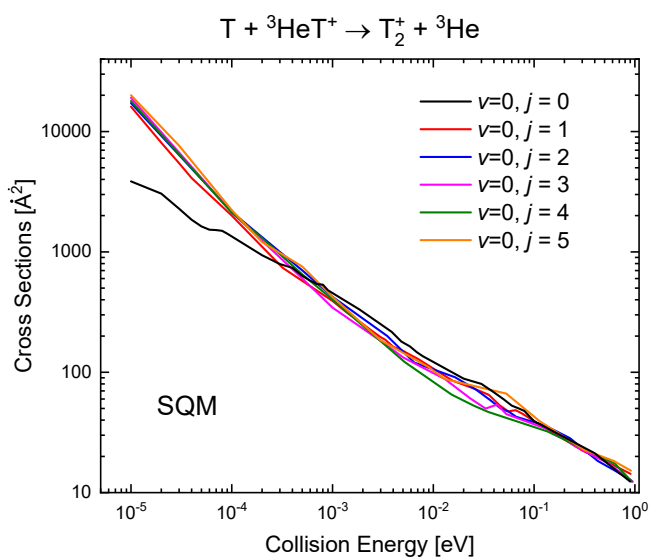


Fig. 2 Integral cross sections obtained with the SQM approach for the $T + {}^3\text{HeT}^+(v=0, j=0-5) \rightarrow T_2^+ + {}^3\text{He}$ reactions.

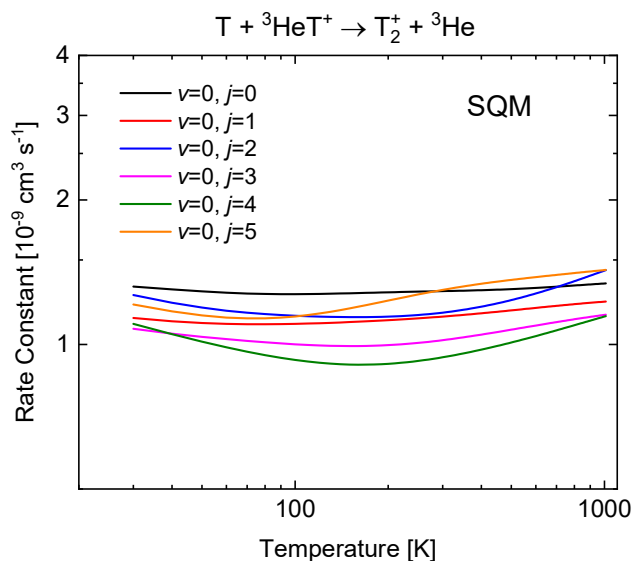


Fig. 4 Rate constants for the $T + {}^3\text{HeT}^+(v=0, j=0-5) \rightarrow T_2^+ + {}^3\text{He}$ reactions obtained from the SQM cross sections shown in Figure 2.

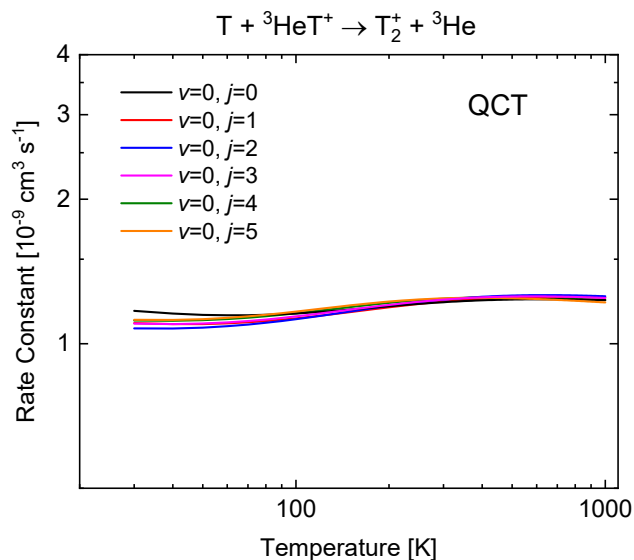


Fig. 5 Rate constants for the $T + {}^3\text{HeT}^+(v=0, j=0-5) \rightarrow \text{T}_2^+ + {}^3\text{He}$ reactions obtained from the QCT cross sections shown in Figure 3.

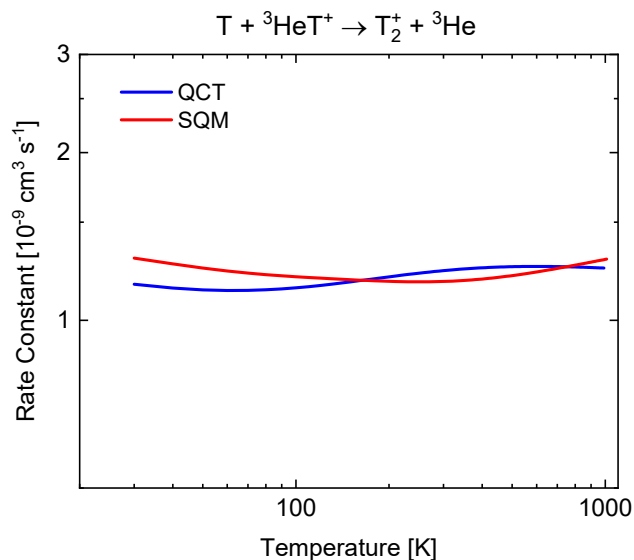


Fig. 6 Comparison between the thermal rate constants obtained from those for the $T + {}^3\text{HeT}^+(v=0, j=0-5) \rightarrow \text{T}_2^+ + {}^3\text{He}$ reactions obtained from the QCT (blue) and SQM (red) rate constants shown in Figures 5 and 4, respectively, by means of the expression $k(T) = e^{-E_j/KT} k_j(T) / \sum_j e^{-E_j/KT}$, where j stands for the corresponding $v=0, j=0-5$ rovibrational state.

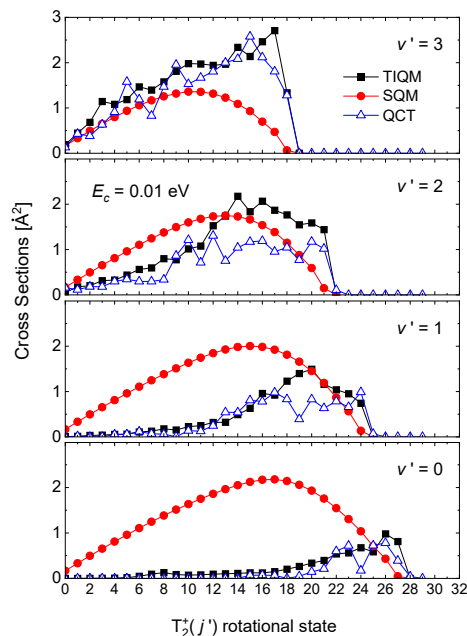


Fig. 7 Rotational distributions (measured in \AA^2) at $E_c = 1 \times 10^{-1}$ calculated with the TIQM (black squares), SQM (red circles) and QCT (blue triangles) approaches for the $T + {}^3\text{HeT}^+(v=0, j=0) \rightarrow \text{T}_2^+(v'=0-3, j') + {}^3\text{He}$ reaction.

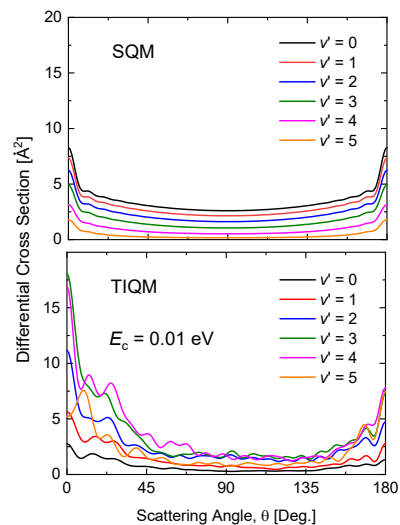


Fig. 8 Final vibrational state solved differential cross sections for the $T + {}^3\text{HeT}^+(v=0, j=0) \rightarrow \text{T}_2^+(v'=0-5) + {}^3\text{He}$ reaction at $E_c = 0.01$, obtained with the SQM (top panel) and TIQM (bottom panel) approaches